

Anna ZIELIŃSKA-JUREK *, Małgorzata WALICKA *, Anna TADAJEWSKA *,
Izabela ŁĄCKA **, Maria GAZDA ***, Adriana ZALESKA *

PREPARATION OF Ag/Cu-DOPED TITANIUM (IV) OXIDE NANOPARTICLES IN W/O MICROEMULSION

Received March 23, 2010; reviewed; accepted May 22, 2010

The Cu-TiO₂ and Ag/Cu-TiO₂ nanoparticles have been prepared using a water-in-oil microemulsion system of water/AOT/cyclohexane. The photocatalytic activity of the catalysts was estimated by measuring the decomposition rate of phenol in 0.21 mM aqueous solution under visible light irradiation. The bioactivity of Ag/Cu-doped titanium (IV) oxide nanocomposites was estimated using bacteria *Escherichia coli* and *Staphylococcus aureus*, yeast *Saccharomyces cerevisiae* and pathogenic fungi belonging to *Candida* family. The photocatalysts' characteristics by X-ray diffraction, BET surface area measurements, Scanning Electron Microscopy (SEM) energy dispersive spectroscopy (EDS) analysis showed that a sample with the highest photo- and bioactivity had anatase structure, about 190 m²/g specific surface area, absorbed light for $\lambda > 400$ nm and contained 1.45 mass % of silver, 1.40 mass % of copper and 59.4 mass % of Ti.

keywords: Ag/Cu-doped TiO₂, microemulsion, heterogeneous photocatalysis, bioactivity

1. INTRODUCTION

Titanium (IV) oxide nanoparticles is one of the most studied semiconductors for

* Department of Chemical Technology, Chemical Faculty, anna_z@chem.pg.gda.pl (A. Zielińska-Jurek)

** Department of Pharmaceutical Technology and Biochemistry, Chemical Faculty

***Department of Solid State Physics, Faculty of Applied Physics and Mathematics, Gdansk University of Technology, 80-233 Gdańsk, Poland

photocatalytic degradation of hazardous and toxic organic pollutants, solar energy conversion, disinfection and self-cleaning coatings. However, the pure TiO₂ has wide band gap and can only be excited by a small UV fraction of solar light and thus this practically limits the use of sunlight or visible light as an irradiation source in photocatalytic reactions on TiO₂.

For the purpose of overcoming these limitations of TiO₂ and to enhance the photocatalytic activity response into the visible part of the spectrum, the surface modification of TiO₂ with various noble metals [1,2,3], transition metals [4,5,6] or non-metallic elements [7,8] have been widely investigated.

The role of loaded metal is trapping and subsequent transfer of photoexcited electrons on TiO₂ surface. The metals deposited or doped on TiO₂ have the high Schottky barriers and thus act as electron traps, facilitating electron-hole separation and promotes the interfacial electron transfer process. Bamwenda et al. compared the photocatalytic activity of Au-TiO₂ and Pt-TiO₂ nanoparticles in process of hydrogen generation. The maximum hydrogen production yield was observed for platinum- and gold-modified titanium (IV) oxide nanoparticles containing 0.3-1 wt% and 1-2 wt % of noble metal respectively [9]. For the preparation of self-cleaning coatings and water/air filters for reduction the spread of infections and improve the hygienic conditions the silver-doped TiO₂ nanoparticles have been widely investigated.

Hamal et al. reported the preparation and characterization of highly active in visible light new nanoparticle photocatalysts based on silver, carbon and sulfur-doped TiO₂. They found that Ag/(C, S)-TiO₂ nanoparticle photocatalysts degrade the gaseous acetaldehyde 10 and 3 times faster than commercial TiO₂ (P25, Degussa) under visible and UV light, respectively [10]. In recent years, Degussa P25 TiO₂ has set the standard for photoreactivity in environmental applications. Degussa P25 is a nonporous 70:30% anatase-to-rutile mixture with a BET surface area of 55± 15 m²/g and crystallite sizes of 30 nm in 0.1 μm diameter aggregates.

Keleher et al. obtained Ag-TiO₂ nanoparticles, which exhibited antimicrobial activity against gram-positive and gram-negative bacterial strains. The zone of inhibition diameters for the Ag-TiO₂ particles was found to be comparable with those of the other antimicrobial agents (tetracycline, chloramphenicol, erythromycin, and neomycin) [11].

Our previous study confirmed that Ag-TiO₂ nanoparticles obtained in w/o microemulsion system exhibited visible light activity and antimicrobial activity against *E. coli*, *St. aureus*, *S. cerevisiae* and pathogenic fungi belonging to *Candida* family [12].

This paper described the Vis-light photocatalytic activity of the Cu-doped TiO₂ and Ag/Cu-doped TiO₂ nanoparticles prepared in w/o microemulsion system. W/O microemulsion contain inverted micellar aggregates consisting of water droplets surrounded by amphiphiles in a continuous nonpolar system. The particle sizes



generated can be controlled by the nanodroplet size of the inner phase of the microemulsion. The effect of metals amount on photocatalytic activity and antimicrobial properties have been widely investigated.

2. EXPERIMENTAL

2.2. Materials and instruments

Titanium isopropoxide (pure p.a.) was purchased from Aldrich and used as titanium source for the preparation of TiO₂ nanoparticles. Silver nitrate (pure p.a.) was provided by POCh and used as the starting material for the silver nanoparticles. Hydrazine anhydrous (50-60%) was purchased from Aldrich and used as reducing agent. Cyclohexane was used as the continuous oil phase, and sodium bis- (2-ethylhexyl) sulfosuccinate (AOT) purchased from Aldrich as the surfactant, 1-hexanol as the cosurfactant and aqueous solution as the dispersed phase. The crystal structures of the Ag/Cu-TiO₂ nanoparticles were determined from XRD pattern measured in the range of $2\theta = 20\text{--}60^\circ$ using X-ray diffractometer (Xpert PRO-MPD, Philips) with Cu target ($\lambda = 1.542 \text{ \AA}$). The XRD analysis of the crystallite size was based on the Scherrer formula: $d = 0.89\lambda / (Be - Bt)\cos\theta$, where λ is the X-ray wavelength, Be indicates the measured breadth of a peak profile, while Bt is the ideal, non-broadened breadth of a peak and θ is the diffraction angle. The value of Bt was estimated on the basis of the measurements performed for a standard sample of polycrystalline Si with large crystalline grains. The accuracy of the grain size analysis has been estimated to be about 20%. The surface morphology was determined using scanning electron microscope (SEM, LEO 1430 VP) equipped with energy dispersive X-ray spectrometer – EDS, Quantax 200. Nitrogen adsorption–desorption isotherms were recorded at liquid nitrogen temperature (77K) on a Micromeritics Gemini V (model 2365) and the specific surface areas were determined by the Brunauer–Emmett–Teller (BET) method.

2.3. Preparation of Cu-doped TiO₂ and Ag/Cu-doped TiO₂ photocatalysts

The microemulsions were prepared by mixing the aqueous solution of metal ions (Ag⁺, Cu²⁺) and N₂H₄·H₂O into the 0.2 M AOT/cyclohexane solution. Cu or Ag/Cu bimetallic nanoparticles were prepared by dropwise addition microemulsion containing the reducing agent (hydrazine) into the microemulsion containing metal precursor in water cores as was shown in Fig. 1. The molar ratio of hydrazine and silver nitrate or copper nitrate was held constant at a value of 3. Water content was controlled by fixing the molar ratio of water to surfactant (w_0) at 2.

Then TiO₂ precursor titanium tetraisopropoxide (0.2M TIP) was added into the



microemulsion containing metal nanoparticles. The concentration of metal precursors, which varied from 0.1 to 6.5 mol% was related to the concentration of TIP in the microemulsion system. During the precipitation nitrogen was bubbled continuously through the solution. The Ag/Cu-TiO₂ particles precipitated were separated, washed with ethanol and deionized water several times to remove the organic contaminants and surfactant. The particles were dried at 80°C for 48 h and were then calcinated at 450°C for 2h.

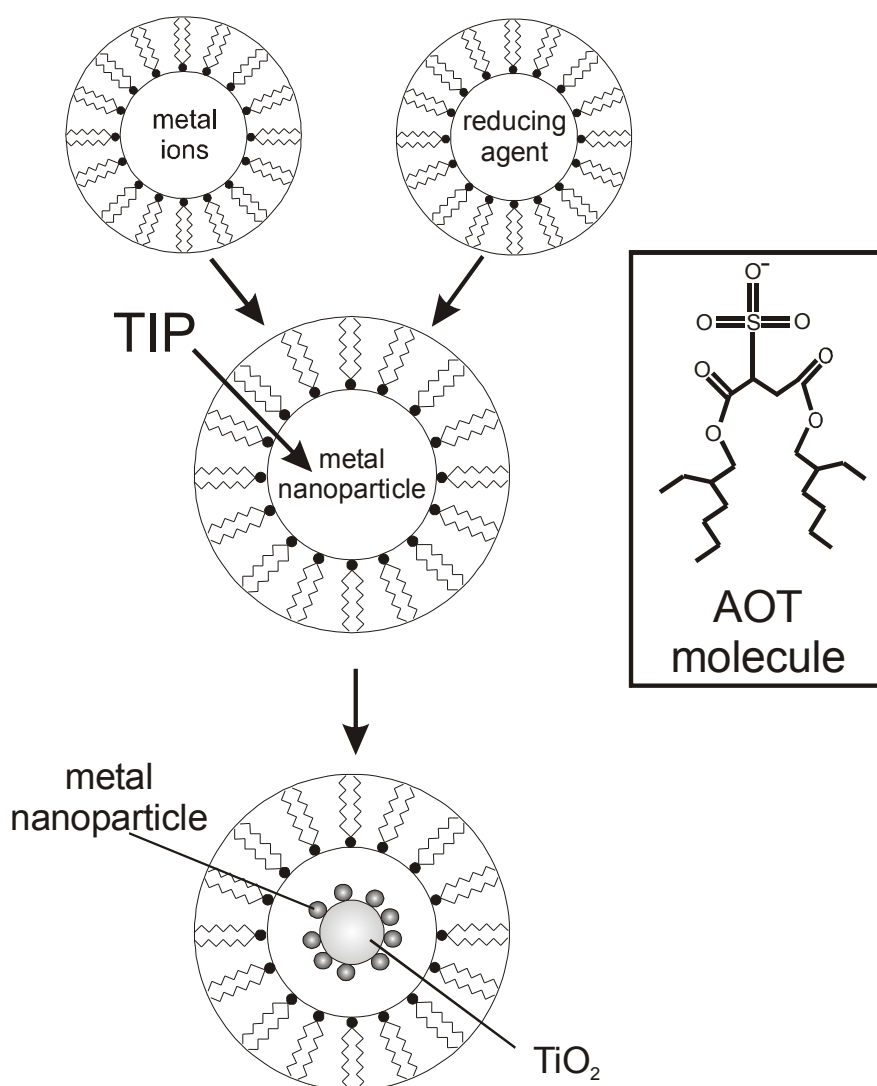


Fig. 1. Mechanism of the preparation method of Ag/Cu-doped titanium (IV) oxide nanoparticles in reverse micelles.

2.4. Measurements of photocatalytic activity

The photocatalytic activity of Ag/Cu-TiO₂ powders under visible light was estimated by measuring the decomposition rate of phenol (0.21 mmol/dm³) in an aqueous solution. Photocatalytic degradation runs were preceded by blind tests in the absence of a photocatalyst or illumination. Phenol was selected as a model pollutant because it is a non-volatile and common contaminant present in industrial wastewaters. The mechanism of phenol decomposition is also well established. 25 ml of phenol solution at concentration of 2.1·10⁻⁴ M containing suspended photocatalyst (125 mg) was stirred using a magnetic stirrer and aerated (5 dm³/h) prior and during the photocatalytic process. Aliquots of 1.0 cm³ of the aqueous suspension were collected at regular time periods during irradiation and filtered through syringe filters (Ø = 0.2 µm) to remove photocatalyst particles. Phenol concentration was estimated by colorimetric method using UV-vis spectrophotometer (DU-7, Beckman). The suspension was irradiated using 1000 W Xenon lamp (6271H, Oriel), which emits both UV and vis light. The optical path included water filter and glass filters (GG400 or UG1, Schott AG) to cut off IR and VIS or UV irradiation, respectively. GG glass filter transmitted light of wavelength greater than 400 nm. The temperature during the experiments was maintained at 10°C.

2.5. Measurements of bioactivity (antibacterial and antifungal)

Bioactivity was measured as a minimal inhibitory concentration (MIC). Antibacterial and antifungal activity was determined by the serial twofold dilution microtiter plate method, in Tryptic Soy Broth medium (TSB, GibcoBRL), for antibacterial activity determination or in YNBG medium (Yeast Nitrogen Base-glucose minimal medium, containing 0,67 % YNB without amino acids and ammonium sulphate with addition of 2 % glucose and 5 g/l of ammonium sulphate, supplemented with uracil at 30 µg/l) for antifungal activity determination. Wells containing serially diluted examined compounds (suspended Ag/Cu-TiO₂) and compound-free controls were inoculated with overnight cultures of tested strains to the final concentration of 10⁴ cfu/ml (colony forming units per ml). The plates were then incubated for 24 h at 37°C (antibacterial activity determination) or at 30°C (antifungal activity determination). The microbial growth was quantified in each well by the measurement of an optical density at λ = 531 nm using the microplate reader (Victor³V, PerkinElmer, Centre of Excellence ChemBioFarm, Faculty of Chemistry, Gdansk University of Technology). MIC (minimal inhibitory concentration) was defined as drug concentration at which at least 80 % decrease in turbidity, relative to that of the compound-free growth control well was found. The antimicrobial activity of Ag/Cu-doped titanium (IV) oxide nanocomposites was estimated using *Escherichia coli* ATCC 10536, *Staphylococcus aureus* ATCC 6538, *Candida albicans* ATCC 10231,



Candida glabrata DSM 11226, *Candida tropicalis* KKP 334, *Saccharomyces cerevisiae* ATCC 9763, *S. cerevisiae* JG and JG CDR1.

3. RESULTS AND DISCUSSION

3.1. XRD analysis

The selected XRD pattern of Ag/Cu-doped TiO₂ powders loaded with different amount of silver are shown in Fig. 2. The average size of anatase crystallites for Ag/Cu-TiO₂ nanoparticles determined from the XRD pattern based on the Scherrer formula was from 8 to 9 nm. Peaks marked “A” and “B” correspond to anatase and brookite phases, respectively. The Ag/Cu-TiO₂_1 and Ag/Cu-TiO₂_3 samples contained anatase and small amount of brookite. The higher silver amount (6.5 mol% of Ag for sample Ag/Cu-TiO₂_4) promote the formation of the pure anatase in preference to anatase/brookite photocatalysts. For the Ag/Cu-TiO₂ powder containing 6.5 mol% of Ag and 0.5 mol% of Cu doped, the peak corresponding to metallic silver at 2 θ = 38.1 was observed. On the contrary for lower dopant amount no additional XRD peaks corresponding to Ag or Cu present can be revealed. This may be attributed to the well dispersion of nanocrystalline metal nanoparticles in the TiO₂ matrix.

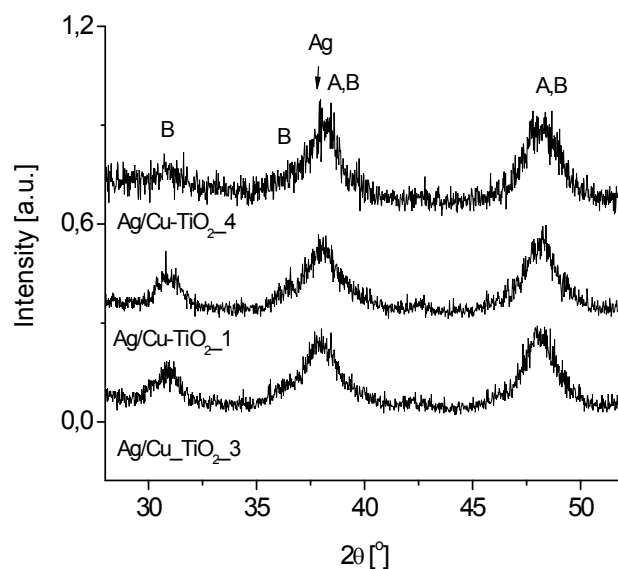


Fig. 2. XRD patterns of Ag/Cu-doped TiO₂ nanoparticles calcinated for 2 hours at 450°C

3.2. BET surface area and microscopy analysis

Table 1 presents the characterization results for the silver and copper doped TiO₂ nanoparticles. The Cu-TiO₂ photocatalyst modified with 4.5 mol.% of Cu has the lowest BET surface area of about 161 m²/g, which was comparable to pure TiO₂ obtained in the same microemulsion system.

Table 1. Characteristics of Ag/Cu- doped TiO₂ prepared in w/o microemulsion

Sample label	Amount of metal precursor [mol %]		Surfactant	Sample color	BET [m ² /g]	Phenol degradation rate [μmol/min] under Vis light (λ > 400nm)
	Cu	Ag				
TiO ₂	0	0	AOT	white	160	0,29
Cu-TiO ₂ _1	0.1	0	AOT	green	195	0.62
Cu-TiO ₂ _2	0.5	0	AOT	green	206	0.94
Cu-TiO ₂ _3	2.5	0	AOT	green	202	0.53
Cu-TiO ₂ _4	4.5	0	AOT	green	161	0.43
Ag/Cu-TiO ₂ _1	0.5	1.5	AOT	yellow	190	2.41
Ag/Cu-TiO ₂ _2	1.5	0.5	AOT	green	209	0.74
Ag/Cu-TiO ₂ _3	0.5	0.5	AOT	yellow	194	1.36
Ag/Cu-TiO ₂ _4	0.5	6.5	AOT	yellow	187	1.22
Ag/Cu-TiO ₂ _5	4.5	0.5	AOT	green	223	0.50
Ag/Cu-TiO ₂ _6	0.5	4.5	AOT	yellow	180	2.25
Ag/Cu-TiO ₂ _7	0.5	2.5	AOT	yellow	186	2.07



For other Cu-TiO₂ and Ag/Cu-TiO₂ samples containing from 0.1 to 4.5 mol.% of Cu and 0.5 to 6.5 mol.% of Ag the surface areas varied from 180 to 223 m²/g. It was observed that metal dopant affects the surface area of TiO₂ powder samples obtained by microemulsion system. The BET areas decrease for increasing Ag concentration more than for increasing Cu amount in the sample. Sample modified with 4.5 mol% of Ag and 0.5 mol% of Cu has the BET surface area of about 180 m²/g.

For sample Ag/Cu-TiO₂_1 containing 1.5 mol.% of Ag and 0.5 mol.% of Cu specific surface area average 190 m²/g and was lower than for Ag/Cu-TiO₂_2 containing 0.5 mol.% of Ag and 1.5 mol.% of Cu with BET surface area average 209 m²/g. However, it is known from the literature that for visible irradiation, the surface area is not as crucial as the size of noble metal, as was already shown for Ag-TiO₂ composites [12]. The obtained results indicated that rather other parameters, such as silver or copper presence, cause their enhancement in photoactivity than the surface area.

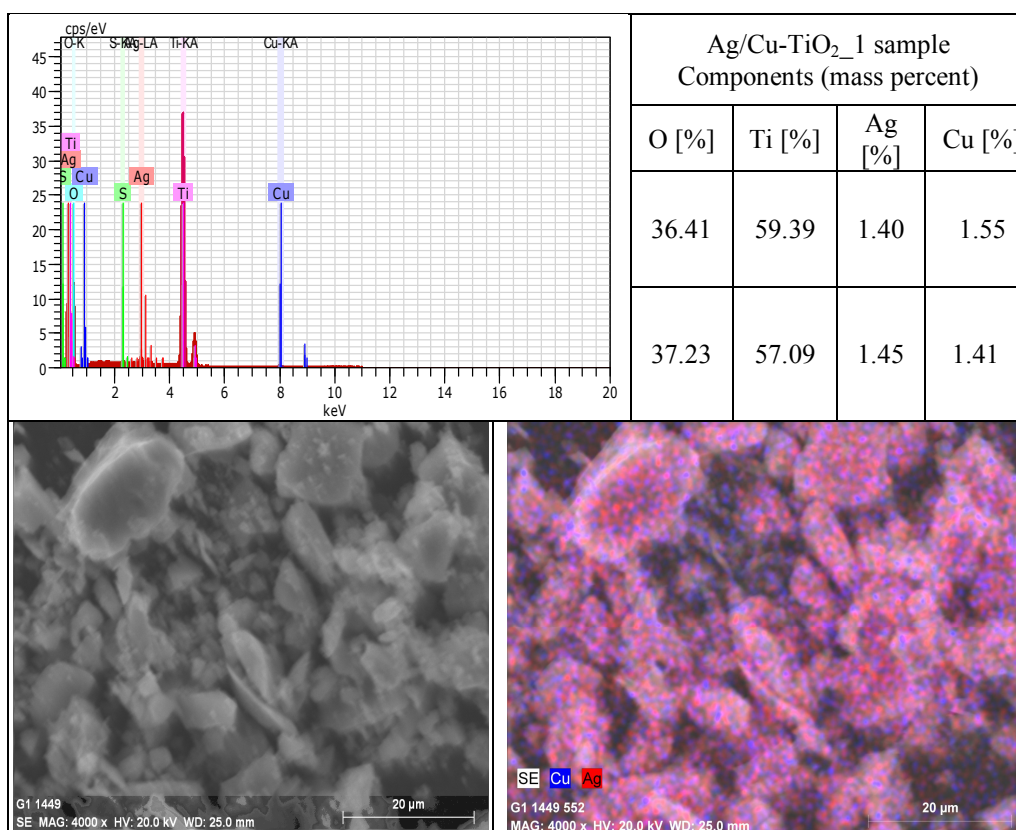


Fig. 3. SEM image and elemental mapping of Ag/Cu-TiO₂_1 nanoparticles prepared by microemulsion method

Microstructures of the obtained nanocomposites and their surface morphologies were studied by SEM equipped with EDS. SEM images and EDS mappings of silver-copper composite material in the TiO₂ matrix for sample Ag/Cu-TiO₂_1 (containing 1.5 mol% of silver and 0.5 mol% of copper) and Ag/Cu-TiO₂_4 (containing 6.5 mol% of silver and 0.5 mol% of copper) are given in Fig. 3. and Fig. 4, respectively. From elemental mapping mode highly and uniformly dispersed Ag/Cu nanoparticles on the TiO₂ support were observed. This implied good interaction between dopant and support in microemulsion preparation method. Since the EDS mapping were scanned from the surface, composition of elements correspond to the surface composition of the structure.

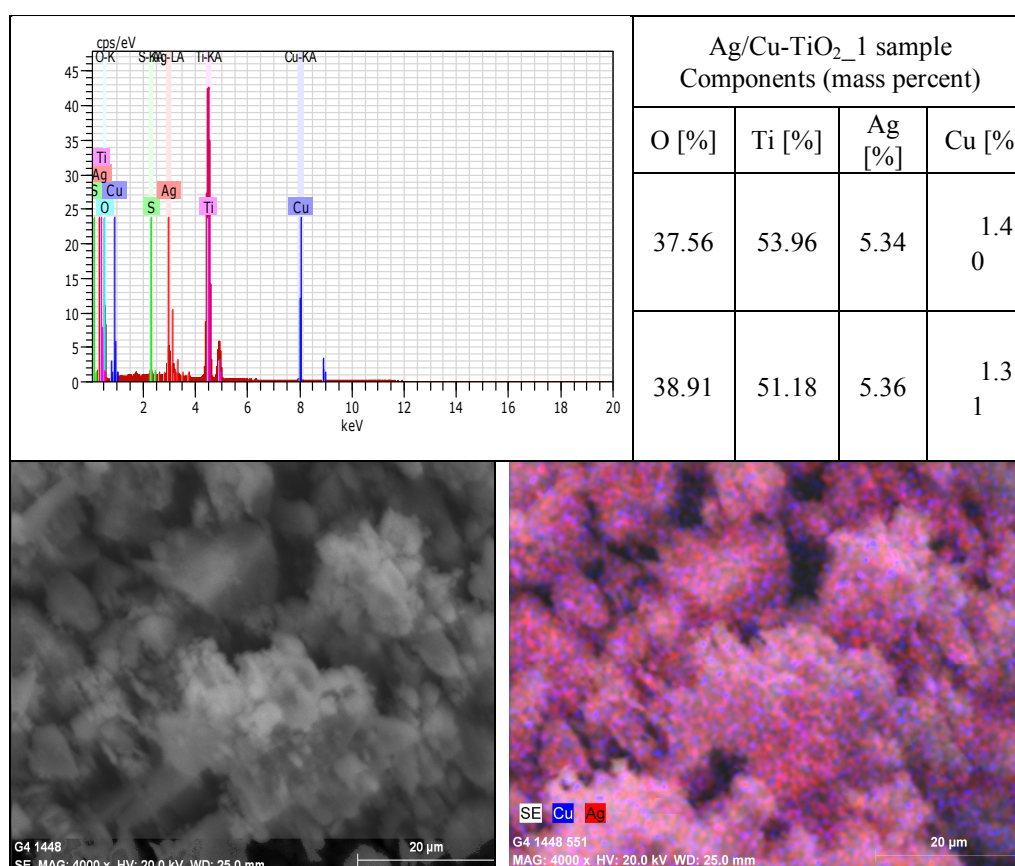


Fig. 4. SEM image and elemental mapping of Ag/Cu-TiO₂_4 nanoparticles prepared by microemulsion method

Since molar ratio of Ag to Cu used during synthesis equaled to 13 and 3 for sample Ag/Cu-TiO₂_4 and Ag/Cu-TiO₂_1, respectively, the higher surface concentration of silver was observed for the sample Ag/Cu-TiO₂_4.

3.3. Photocatalytic activity of Cu-TiO₂ and Ag/Cu-doped TiO₂ under visible light

The photocatalytic activity of the metal-doped TiO₂ nanoparticles was evaluated by measuring the decomposition of phenol. No phenol was degraded in the absence of illumination indicating that there was no dark reaction at the surface of Cu-TiO₂. Also the reference test in the absence of photocatalysts under visible light showed the lack of phenol degradation. The efficiency of phenol degradation after 80 min. illumination by visible light in the presence of Cu-TiO₂ nanoparticles are presented in Table 1. The rate of phenol degradation as a function of mol% of Cu is presented in Fig. 5. The photodegradation efficiency under visible light increased with the increase in the copper loading up to 0.5 mol % and then decreased. The rate of phenol decomposition measured in the presence of the sample Cu-TiO₂_2 after 60 min. of irradiation average 0.94 μmol/min. Thus, it was observed that optimum Cu loading for this preparation method was between 0.5 and 1.0 mol.%. Our results are in good agreement with others. Xin. et al. observed that over 0.06 mol% Cu-TiO₂, the degradation of RhB ratio is the highest. The Cu-TiO₂ photocatalyst containing about 0.06 mol% of Cu possess abundant electronic trap, which effectively inhibits the recombination of photoinduced charge carriers, improving the photocatalytic activity of TiO₂ [13].

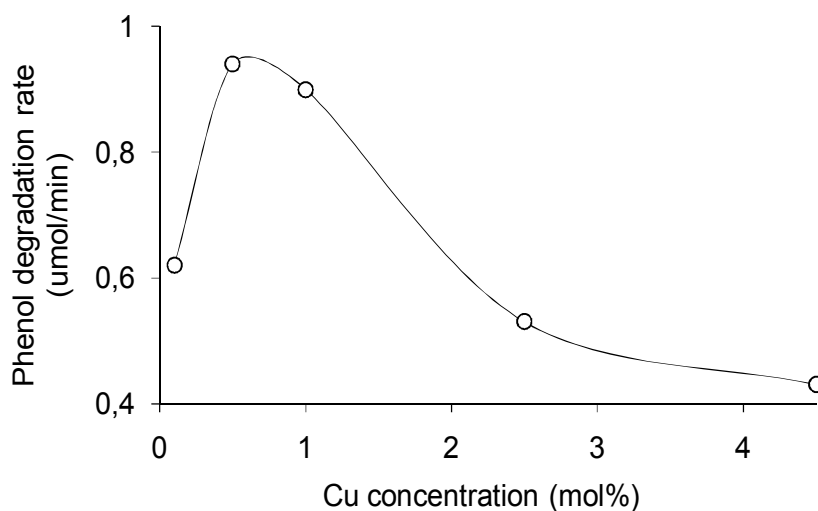


Fig. 5. Degradation rate for phenol v.s. mol% of Cu/TiO₂



For the purpose of increasing the efficiency of phenol degradation under visible light the bimetallic Ag/Cu and Au/Cu nanoparticles were prepared for modification of TiO₂ surface. Previously we have also obtained Ag/Au-modified TiO₂ nanoparticles which exhibited higher photodegradation rate in visible region than both Ag-TiO₂ and Au-TiO₂ photocatalysts. Therefore the synergistic effect of gold and silver nanoparticles on photocatalytic activity of Cu-TiO₂ nanoparticles in visible light was also expected. The efficiency of phenol degradation in the presence of pure TiO₂ and Ag/Cu-doped TiO₂ nanoparticles are presented in Table 1 and Fig. 6.

The maximum in the photocatalytic activity under visible light was observed for sample containing 0.5 mol % of Cu and 1.5 mol% of Ag. The rate of phenol decomposition average 2.41 $\mu\text{mol}/\text{min}$ and was higher than for Ag/Cu-TiO₂_2 containing 1.5 mol% of Cu and 0.5 mol% of Ag. It indicates that silver present was more beneficial for visible light activation of TiO₂ doped photocatalysts than higher copper amount.

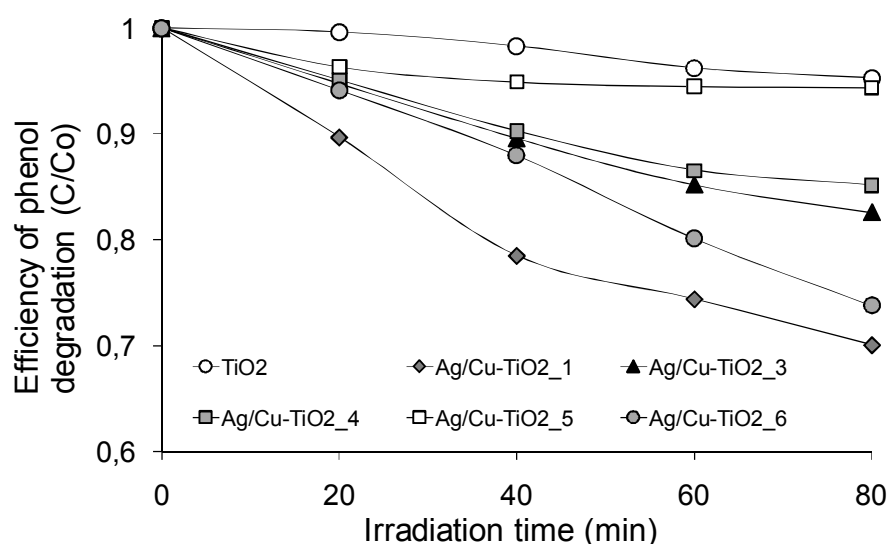


Figure 6. Efficiency of phenol photodegradation in the presence of Ag/Cu-doped TiO₂ under visible light ($\lambda > 400$ nm). Experimental conditions: $C_0 = 0.21$ mM, $m(\text{TiO}_2) = 125$ mg, $T = 10^\circ\text{C}$, $Q_{\text{air}} = 5$ l/h

Compared to Ag/Cu-TiO₂_1 photocatalyst the degradation rate decreased to 2.25 $\mu\text{mol}/\text{min}$, 1.36 $\mu\text{mol}/\text{min}$ and 1.22 $\mu\text{mol}/\text{min}$ for the Ag/Cu-TiO₂ containing 4.5 mol%, 0.5 mol% and 6.5 mol% of silver, respectively. The Au/Cu-TiO₂ nanoparticles revealed lower photocatalytic activity compared to Ag/Cu-TiO₂ photocatalysts containing the same metal amount loading on TiO₂ surface (see Table 1 samples Ag/Cu-TiO₂_3 and Au/Cu-TiO₂_1).

3.4. Antimicrobial susceptibility testing method (MIC)

It has been well known that silver and copper possesses strong antibacterial activities both as metal nanoparticles and ions. Determining the MIC values of antibacterial agents is a valuable means for comparing the antibacterial effectiveness of the agents. The MIC values were the lowest concentration of Cu-TiO₂ and Ag/Cu-TiO₂ in aqueous solution that inhibited visual growth after 24 h of incubation. Thus, lower MIC value means higher bioactivity.

Table 2. Minimum inhibitory concentration (MIC) of Ag/Cu-doped TiO₂ nanoparticles

Type of micro organism	Microbial Strains	MIC for Ag/Cu-TiO ₂ [μg/ml]						MIC for Cu-TiO ₂ [μg/ml]				TiO ₂
		1	2	3	4	5	6	1	2	3	4	
Yeast	<i>Candida albicans</i> ATCC 10231	250	500	500	125	1000	250	>1000	>1000	>1000	>1000	>1000
	<i>Candida glabrata</i> DSM 11226	250	500	500	125	1000	250	>1000	>1000	>1000	>1000	>1000
	<i>Candida tropicalis</i> KKP 334	250	500	500	62	500	125	>1000	>1000	>1000	>1000	>1000
	<i>Saccharomyces cerevisiae</i> ATCC 9763	62	250	250	31	500	125	1000	500	>1000	>1000	>1000
	<i>Saccharomyces cerevisiae</i> JG	62	125	125	16	250	125	1000	>1000	>1000	>1000	>1000
Bacteria	<i>Escherichia coli</i> ATCC 10536	250	500	500	62	1000	250	>1000	>1000	>1000	>1000	>1000
	<i>Staphylococcus aureus</i> ATCC 6538	250	500	500	62	1000	250	>1000	>1000	>1000	>1000	>1000

The minimal inhibitory concentration of microorganism growth for as-prepared Ag/Cu-TiO₂ nanocomposites was estimated using bacteria *Escherichia coli* and *Staphylococcus aureus*, yeast *Saccharomyces cerevisiae* and pathogenic fungi belonging to *Candida* family. The effect of silver and copper loading on MIC value is presented in Table 2. For Cu-TiO₂_5 loaded with 4.5 mol.% of Cu, the inhibition in microorganisms growth was not observed even for photocatalyst concentration below 500 μg/ml. The minimal inhibition concentration differed from 62 to 1000 μg/ml, depending on microbial strain and metal concentration. The photocatalysts doped with

silver revealed higher antimicrobial activity than pure TiO₂ obtained in microemulsion system or samples containing only copper nanoparticles deposited on TiO₂ surface. It indicated that silver possess higher antimicrobial activity than copper nanoparticles prepared in microemulsion system. The best antimicrobial activity revealed Ag/Cu-TiO₂_4 with highest silver amount average 6.5 mol% and sample Ag/Cu-TiO₂_1 containing 1.5 mol% of Ag and 0.5 mol% of Cu, which exhibited also the highest efficiency of phenol degradation under visible light as shown in Table 1 and Fig. 6.

4. CONCLUSIONS

The Cu-TiO₂ and Ag/Cu-TiO₂ nanoparticles have been prepared using a water-in-oil microemulsion system of water/AOT/cyclohexane. It was found that obtained nanocomposites contained highly and uniformly dispersed Ag/Cu nanoparticles on the TiO₂ surface. XRD and the BET measurements corroborate that these doped materials are made up of the anatase crystalline phase and have high surface areas fluctuating from 161 to 223 m²/g depending on metal loading on TiO₂ surface. The photodegradation efficiency under visible light increased with the increase in the copper loading up to 0.5 mol % and then decreased. The maximum in the photocatalytic activity under visible light was observed for sample containing 0.5 mol % of Cu and 1.5 mol% of Ag. The rate of phenol decomposition average 2.41 μmol/min. The antimicrobial susceptibility was tested using bacteria *Escherichia coli* and *Staphylococcus aureus*, yeast *Saccharomyces cerevisiae* and pathogenic fungi belonging to *Candida* family. The photocatalysts doped with silver revealed higher antimicrobial activity than samples containing only copper nanoparticles deposited on TiO₂ surface. It indicated that silver possesses higher antimicrobial activity than copper nanoparticles prepared in the same microemulsion system. This study suggested that Ag/Cu-TiO₂ nanoparticles can be used as effective antimicrobial agent for reduction the spread of infections in commercial facilities.

ACKNOWLEDGMENTS

This research was financially supported by Polish Ministry of Science and Higher Education grant No. N N507 272136, by the European Union in the framework of the European Social Fund. The system project of the Pomorskie Voivodeship "InnoDoktorant - Scholarships for PhD students, II edition.

REFERENCES

- [1] K. KAWAHARA, K. SUZUKI, Y. OHKO, T. TATSUMA, *Phys . Chem. Chem. Phys .* 7 (2005) 3851 – 3855.
- [2] KOWALSKA E., ABE R., OHTANI B., *Chem. Commun.*, 2 (2009), 241-43
- [3] ISHIBAI Y., SATO J., NISHIKAWA T., MIYAGISH S., *Appl. Catalal. B: Environmental*, 79 2 (2008) 117-121
- [4] COLÓN G., MAICU M., HIDALGO M.C., NAVIÓ J.A., *Appl. Catal. B: Environmental* 67 (2006) 41–51
- [5] SONAWANE R.S., KALE B.B., DONGARE M.K., *Materials Chemistry and Physics* 85 (2004) 52–57
- [6] IKEDA S., SUGIYAMA N., PAL B., MARCI G., PALMISANO G., NOGUCHI H., UOSAKI K., OHTANI B., *Phys . Chem. Chem. Phys.*, 3 (2001) 267-273
- [7] ZALESKA A., SOBCZAK J.W., GAZDA M., GRABOWSKA E., HUPKA J, *Appl. Catal. B* 469-475
- [8] GÓRSKA P., ZALESKA A., HUPKA J., *Sep Purif. Technol.* 68 (2009) 90· 96
- [9] BAMWENDA G.R., TSUBOTA S., NAKAMURA T., HARUTA M., *J. Photochem. and Photobio. A: Chem.*, 89 (1995) 177
- [10] HAMAL D. B., K. J. KLABUNDE, *J. Colloid Interf. Sci.* 311 (2007) 514–522.
- [11] KELEHER J., BASHANT J., HELDT N., JOHNSON L. and LI Y., *World J. Microbiol. Biotechnol.* 18 (2002) 133–139.
- [12] ZIELIŃSKA A., KOWALSKA E., SOBCZAK J.W., ŁACKA I., GAZDA M., OHTANI B., HUPKA J., ZALESKA A., *Sep. Purif Technol.* (2010) doi 10.1016/j.seppur.2010.03.002
- [13] XIN B., WANG P., DING D., LIU J., REN Z., FU H., *Appl Surf Sci*, 254 (2008) 2569–2574.

